

## Far-Infrared Absorption and the Metal-to-Insulator Transition in Hole-Doped Cuprates

S. Lupi,<sup>1</sup> D. Nicoletti,<sup>1</sup> O. Limaj,<sup>1</sup> L. Baldassarre,<sup>1</sup> M. Ortolani,<sup>1</sup> S. Ono,<sup>2</sup> Yoichi Ando,<sup>3</sup> and P. Calvani<sup>1</sup>

<sup>1</sup>CNR-INFM Coherentia and Dipartimento di Fisica, Università di Roma “La Sapienza,” Piazzale A. Moro 2, I-00185 Roma, Italy

<sup>2</sup>Central Research Institute of Electric Power Industry, Komae, Tokyo 201-8511, Japan

<sup>3</sup>Institute of Scientific and Industrial Research, Osaka University, Ibaraki, Osaka 567-0047, Japan

(Received 23 December 2008; published 21 May 2009)

By studying the optical conductivity of  $\text{Bi}_2\text{Sr}_{2-x}\text{La}_x\text{CuO}_6$  and  $\text{Y}_{0.97}\text{Ca}_{0.03}\text{Ba}_2\text{Cu}_3\text{O}_6$ , we show that the metal-to-insulator transition in these hole-doped cuprates is driven by the opening of a small gap at low  $T$  in the far infrared. Its width is consistent with the observations of angle-resolved photoemission spectroscopy in other cuprates, along the nodal line of the  $k$  space. The gap forms as the Drude term turns into a far-infrared absorption, whose peak frequency can be approximately predicted on the basis of a Mott-like transition. Another band in the midinfrared softens with doping but is less sensitive to the metal-to-insulator transition.

DOI: 10.1103/PhysRevLett.102.206409

PACS numbers: 71.30.+h, 74.25.Gz, 78.30.-j

The parent compounds of high- $T_c$  cuprates are half-filled antiferromagnetic (AFM) insulators where the Coulomb repulsion opens a wide charge-transfer (CT) gap ( $\geq 1.5$  eV) in the excitation spectrum. By adding a few percent holes ( $p$ ) or electrons ( $n$ ) per Cu ion, the CT gap is filled by a broad infrared absorption, while angle-resolved photoemission spectroscopy (ARPES) reveals fully gapped single particle excitations at low temperature [1]. At  $p \geq 0.05$ , like in  $\text{La}_{2-x}\text{Sr}_x\text{CuO}_4$  (LSCO), or  $n \geq 0.12$ , like in  $\text{Nd}_{2-x}\text{Ce}_x\text{CuO}_4$  (NCCO), the insulator eventually turns at low  $T$  into a superconductor and above  $T_c$  into a “strange metal” characterized by a pseudogap in the density of states [2]. Much effort has been devoted in the past two decades to understand these three phases and their excitation spectrum. However, less attention has been paid to the mechanism of the transition from the AFM insulator to the strange metal and vice versa, which is far from being clear. For example, the onset of a metallic state is observed at  $p$  or  $n$  values much higher than those which destroy the AFM long range order [3]. Therefore, magnetism should not play a dominant role in the metal-to-insulator transition (MIT). The mechanisms responsible for the localization of the carriers then may be disorder due to dopant ions [4], local electron-spin interactions [5], or the electron-phonon coupling [6].

In the present Letter, we investigate the MIT by studying the behavior of the optical conductivity  $\sigma_1(\omega)$  across the transition, in the single Cu-O layer cuprate  $\text{Bi}_2\text{Sr}_{2-x}\text{La}_x\text{CuO}_6$  (BSLCO). Therein, hole doping can be accurately controlled like in LSCO by replacing Sr by La. In BSLCO,  $p$  decreases [7] for increasing  $x$  according to a relation which is not linear, due to compensation effects, but well known [8,9]. Finally,  $T_c$  is low enough ( $\approx 30$  K at optimum doping) to allow for a study of the normal state of the Cu-O planes at low  $T$ . Here we have measured four single crystals [9] with  $x = 1.0, 0.9, 0.8,$  and  $0.7$ , corresponding to  $p \approx 0.03, 0.07, 0.10,$  and  $0.12$ , respectively. At

$x = 1.0$ , one reaches the lowest  $p \approx 0.03$  allowed by the miscibility of La in the  $\text{Bi}_2\text{Sr}_2\text{CuO}_6$  matrix. Therefore, we have also measured a single crystal of  $\text{Y}_{1-x}\text{Ca}_x\text{Ba}_2\text{Cu}_3\text{O}_6$  (YCBCO) with  $x = 0.03$  and  $p \approx 0.015$ . As in YCBCO the CuO chains are empty and only the Cu-O plane contributes to the  $ab$  optical response [10], we could thus probe five Cu-O planes with decreasing hole doping, from an underdoped metallic state ( $p \approx 0.12$ ) to an AFM insulating phase ( $p \approx 0.015$ ).

The  $ab$ -plane resistivity  $\rho_{ab}(T)$  of the four BSLCO crystals is reported in the insets in Fig. 1, and dc conductivity values are shown, for selected temperatures, on the vertical axis of the same figure. In *a*, for  $p \approx 0.12$ ,  $\rho_{ab}(T)$  shows a metallic behavior above the superconducting transition at  $T_c = 13$  K. The crystal with  $p \approx 0.10$  in Fig. 1(b) displays a metallic behavior above 50 K and a broad minimum above the transition to a superconducting state [9] at  $T_c \approx 1.4$  K. At  $p \approx 0.07$ ,  $\rho_{ab}(T)$  in *c* is nearly constant down to  $\sim 50$  K. Below, it diverges for  $T \rightarrow 0$  according to a variable range hopping regime [9]. A clearly semiconducting behavior at any  $T$  ( $d\rho_{ab}/dT < 0$ ) is instead shown by the compound with  $p \approx 0.03$  in Fig. 1(d). Therefore the MIT can be placed between  $p \approx 0.10$  and  $p \approx 0.07$ . This finding is consistent with the Mott-Ioffe-Regel limit, which fixes the metal-to-insulator crossover and, for the Cu-O planes, can be written as [11]  $k_F l = (hc_0/e^2\rho_{ab}) \sim 1$ . Here  $k_F$  is the Fermi wave vector,  $l$  is the carrier mean free path, and  $c_0$  is the  $c$ -axis lattice spacing. Indeed, following Ref. [7], from the  $\rho_{ab}$  (10 K) in Fig. 1, one obtains  $k_F l = 3.4$  at  $p = 0.10$  and  $k_F l = 0.05$  at  $p = 0.07$ . Magnetic fields on the order of 60 T displace the MIT [7] to  $p \approx 1/8$ .

The  $ab$ -plane reflectivity  $R(\omega)$  of the five samples was measured at near-normal incidence from 40 or 50 to 22 000  $\text{cm}^{-1}$  at different  $T > T_c$ , shortly after cleaving the sample. The real part of the optical conductivity  $\sigma_1(\omega)$ , as obtained from  $R(\omega)$  via Kramers-Kronig trans-

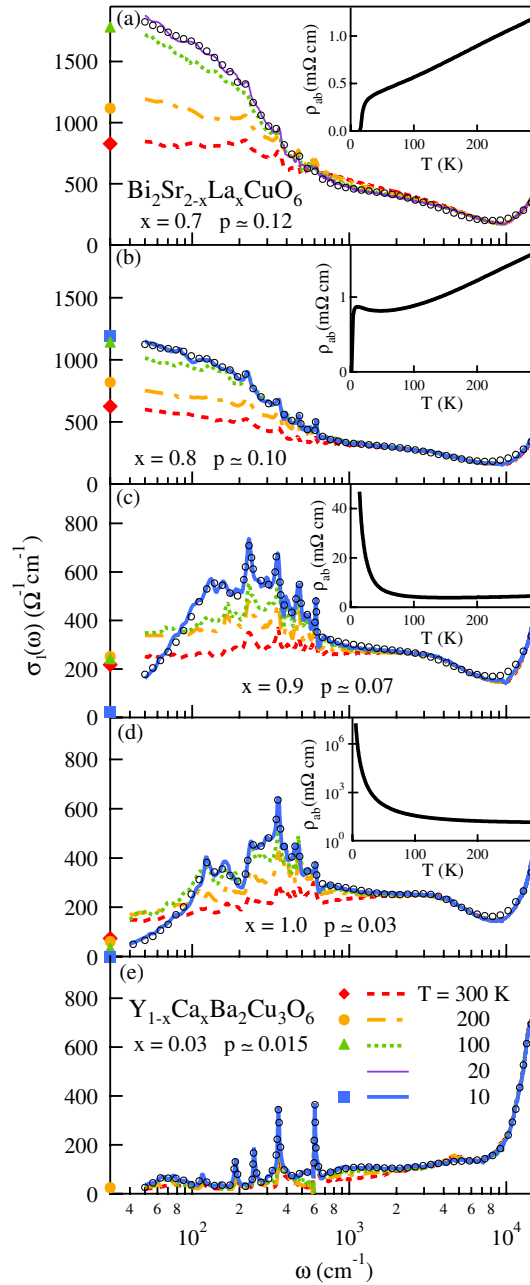


FIG. 1 (color online). Real part of the optical conductivity of  $\text{Bi}_2\text{Sr}_{2-x}\text{La}_x\text{CuO}_6$  with different hole doping  $p$ , and of  $\text{Y}_{0.97}\text{Ca}_{0.03}\text{Ba}_2\text{Cu}_3\text{O}_6$ , at selected temperatures. The circles show examples of the fits used to subtract the phonon contributions in Fig. 2. The symbols on the vertical axis indicate the dc conductivity measured in the same samples at the same  $T$  [ $\sigma_{dc}$  at 20 K is out of the scale of panel (a)]. Full  $ab$ -plane resistivity curves are reported for BSLCO in the insets. The  $\sigma_{dc}$  of YCBCO was measured at 200 K only.

formations, is shown in Fig. 1. The extrapolations to high frequency were based on the data of Ref. [12] and those to zero frequency on Drude-Lorentz fits, which provided deviations from the measured  $\sigma_{dc}(T)$  of a few percent. Afterwards, the extrapolations were adjusted to  $\sigma_{dc}(T)$  [including that at 20 K in Fig. 1(a), not shown]. In insulat-

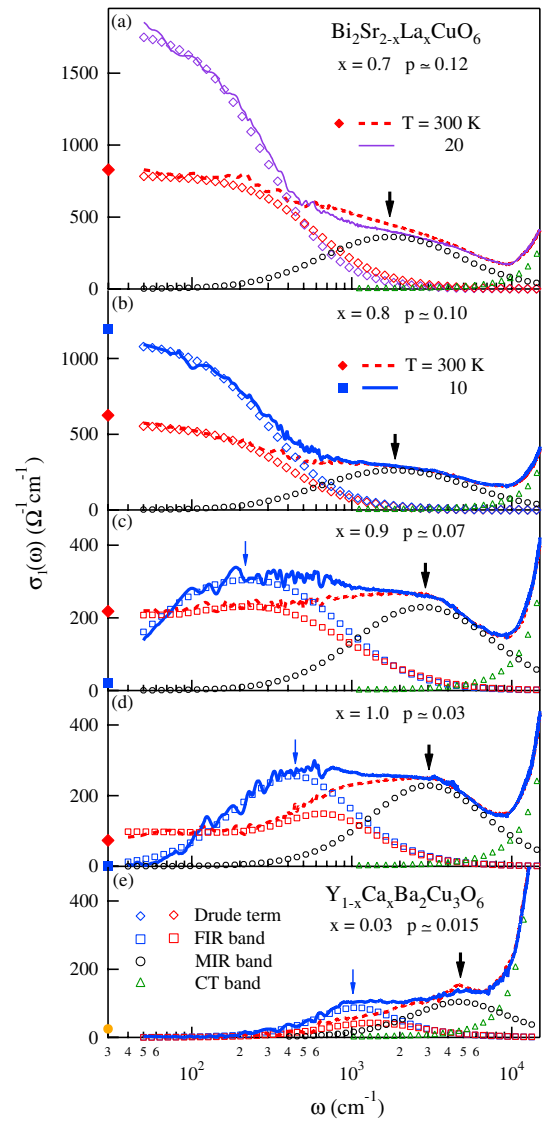


FIG. 2 (color online). Real part of the optical conductivity of the  $\text{Bi}_2\text{Sr}_{2-x}\text{La}_x\text{CuO}_6$  and  $\text{Y}_{0.97}\text{Ca}_{0.03}\text{Ba}_2\text{Cu}_3\text{O}_6$  crystals at two temperatures, after subtraction of the phonon contributions via Lorentzian fits (solid and dashed lines). Open symbols indicate the Lorentzian contributions listed in panel (e), which were identified by fits to the subtracted data (not shown for clarity). In (c) and (d), the FIR band at 300 K includes a weak term peaked at  $\omega = 0$ . MIR and CT bands do not change with temperature. Thin and thick arrows indicate  $\omega_{\text{FIR}}$  and  $\omega_{\text{MIR}}$ , respectively. The dc values are the same as in Fig. 1.

ing YCBCO, a check value of  $\sigma_{dc}$  was measured at 200 K [13] and reported in Fig. 1(e). Figures 1(a) ( $p \approx 0.12$ ) and 1(b) ( $p \approx 0.10$ ) exhibit a Drude term which partially shields the phonon peaks. These are instead well evident in Figs. 1(c) ( $p \approx 0.07$ ), 1(d) ( $p \approx 0.03$ ), and 1(e) ( $p \approx 0.015$ ). Their frequencies are in good agreement with those previously measured [14] on  $\text{Bi}_2\text{SrLaCuO}_y$  and  $\text{YBa}_2\text{Cu}_3\text{O}_y$ . Around  $10000 \text{ cm}^{-1}$ ,  $\sigma_1(\omega)$  increases steeply due to the CT transition between Cu  $3d$  and O  $2p$  orbitals, as in the other cuprates.

Let us now focus on the broad far- and midinfrared contributions in Fig. 1. To better understand their behavior with doping and temperature, in Fig. 2,  $\sigma_1(\omega)$  is reported at 300 K (dashed lines) and at the lowest  $T$  (solid lines), after the phonon lines have been subtracted by accurate Lorentzian fits (those at the lowest  $T$  are shown in Fig. 1). Further fits—not reported in Fig. 2 as they could be hardly distinguished from the data—were then made on the subtracted spectra, by using a Drude term and two broad bands at  $\omega_{\text{FIR}}$  and  $\omega_{\text{MIR}}$  (open symbols). In the metallic phase [Figs. 2(a) and 2(b)] at all temperatures, data are fit by a simple Drude term plus a  $T$ -independent midinfrared (MIR) band peaked at  $\omega_{\text{MIR}} \sim 2000 \text{ cm}^{-1}$ . As  $p$  decreases below the critical hole content  $p_{\text{MIT}}$  [Fig. 2(c)], the Drude term turns at low  $T$  into a far-infrared (FIR) band peaked at  $\omega_{\text{FIR}} \sim 200 \text{ cm}^{-1}$ . Correspondingly,  $\sigma_{dc}$  becomes vanishingly small. At  $p \approx 0.03$  [Fig. 2(d)], a gap  $\sim 100 \text{ cm}^{-1}$  opens in  $\sigma_1(\omega)$  at  $T = 10 \text{ K}$ . Meanwhile,  $\omega_{\text{FIR}}$  shifts to  $\sim 400 \text{ cm}^{-1}$ . Finally, at  $p \approx 0.015$  in Fig. 2(e), the insulating gap extends along the whole far-infrared region, and the FIR peak is displaced to  $\sim 1000 \text{ cm}^{-1}$ . At 300 K, in both Figs. 2(c) and 2(d) the FIR band includes a background—suggestive of incoherent charge transport—which extends to  $\omega = 0$  and accounts for the residual dc conductivity of these samples at room temperature.

The results of Fig. 2 can be compared with those of ARPES experiments. Figure 3 reproduces that in Ref. [1], which shows the gap  $\Delta$  at low doping and low  $T$  in the density of states of different cuprates, measured at the leading edge midpoint along the nodal line of the Brillouin zone. In BSLCO with  $p \approx 0.05$  and  $p \approx 0.07$ , a low- $T$  suppression of the spectral weight was also observed along that direction in the  $k$  space, but the gap width could not be measured for lack of resolving power [15]. We have also plotted in Fig. 3 both the present determinations of the

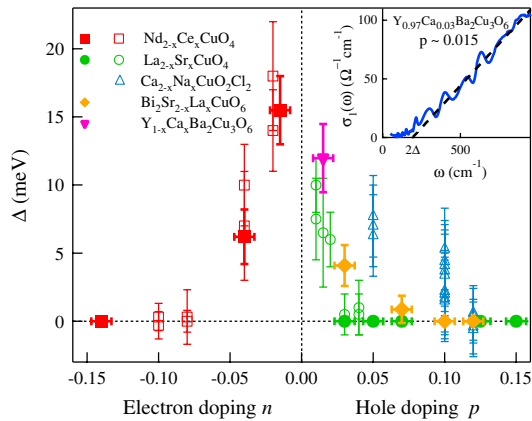


FIG. 3 (color online). Comparison between the gap  $\Delta$  detected in several insulating cuprates by ARPES [1] (open symbols) and by IR spectroscopy (full symbols). Data on BSLCO and YBCO are extracted from Fig. 2, those on NCCO from Ref. [17], and those on LSCO from Ref. [16], by linearly extrapolating the gap edge to  $\sigma_1 = 0$  (see an example in the inset).

gap in BSLCO and YBCO and those extracted from previous measurements in LSCO [16] and in NCCO [17]. In all cases, the infrared gap  $2\Delta$  is obtained after phonon subtraction, by a linear extrapolation to zero [18] of the optical conductivity along the gap edge (see an example in the inset) and then divided by two (by assuming full hole-electron symmetry). If also the IR gap were taken at midheight, the full symbols would displace toward high frequencies by about a factor of 2. In Fig. 3, independently of the procedure employed, both the infrared and ARPES observations consistently indicate that a small gap—just a few meV wide—opens in the density of states at the MIT. In LSCO, however, for reasons which deserve further investigations, the ARPES gap is not observed in the infrared [16,19]. In turn, the band at  $\omega_{\text{MIR}}$  can be associated with the incoherent background observed at  $\sim 0.5 \text{ eV}$  below the quasiparticle peak in the antinodal ARPES spectra of cuprates [1,15,20].

The mechanism of the MIT in the Cu-O plane appears clearly in Fig. 2: As  $p$  decreases below  $p_{\text{MIT}}$ , the carriers increasingly localize at low  $T$  into states having an optical ionization energy  $E_0$  measured by  $\omega_{\text{FIR}}$ .  $E_0$  increases for decreasing  $p$  and reaches about 0.12 eV in the limit of high dilution [Fig. 1(e)]. This value is in excellent agreement with previous observations in electron-doped NCCO at the lowest doping [21].

A simple calculation can predict  $E_0$ . Indeed, as usually done in semiconductors [22], one may model the charge injected in the Cu-O plane as a hole orbiting with radius  $R$  either around a defect or an impurity (in the case of disorder) or within an attractive potential well due to lattice distortion (in a polaronic model).  $E_0$  is related to  $R$  through the hydrogenlike equation

$$E_0 = \left(\frac{3}{2} \frac{a_0}{R}\right)^2 \mathcal{R}, \quad (1)$$

where  $a_0 = 0.0529 \text{ nm}$  is the Bohr radius and  $\mathcal{R} = 109737 \text{ cm}^{-1}$  is the Rydberg constant. The Mott transition occurs at a 2D critical density of holes per Cu ions  $p_{\text{MIT}}$  such that [23] the orbits of adjacent charges overlap in the Cu-O planes. This condition implies that the hole density  $\rho_{\text{MIT}} \sim \frac{1}{\pi R^2}$  and the Cu density  $\rho_{\text{Cu}} = 1/a^2$  satisfy the relation

$$p_{\text{MIT}} = \rho_{\text{MIT}}/\rho_{\text{Cu}} \sim \frac{a^2}{\pi R^2}. \quad (2)$$

Here we use  $a = 0.386 \text{ nm}$ , averaged between the Cu-O lattice parameters of [14]  $\text{Bi}_2\text{SrLaCuO}_y$  and  $\text{YBa}_2\text{Cu}_3\text{O}_y$  (0.383 and 0.389 nm, respectively). Assuming from Fig. 2  $p_{\text{MIT}} \approx 0.08$  and an average  $\rho_{\text{Cu}} = 6.7 \text{ nm}^{-2}$ , one obtains, from Eq. (2),  $R \approx 0.77 \text{ nm}$  and, from Eq. (1),  $E_0 \approx 1150 \text{ cm}^{-1}$ . This value is in very good agreement with the  $\omega_{\text{FIR}} \approx 1000 \text{ cm}^{-1}$  observed here at high hole dilution [in the YBCO with  $p \approx 0.015$  of Fig. 2(e)].

Therefore, one should find the origin of the FIR band in order to understand the MIT mechanism. A first candidate

is disorder. In cuprates doped with Zn impurities or irradiated by high-energy particles, the metallic phase can be destroyed and the Drude spectral weight strongly reduced, due to a poor screening of the impurities and to the resulting fluctuating potentials in the Cu-O planes [24,25]. Recent calculations [4] show that such disorder effects are amplified in a  $d$ -wave electronic symmetry and that, for increasing impurity content, the Drude term turns into a FIR peak at a finite frequency. This framework is consistent with the behavior of BSLCO, where the insulating phase is reached by adding La impurities, not with that of LSCO, which is opposite upon addition of Sr impurities. It seems then that the parameter which governs the metal-to-insulator transition is  $p$  rather than  $x$ .

A different scenario can then be invoked to explain the MIT. Indeed, in BSLCO the FIR peak behaves with  $p$  like a FIR band of NCCO vs  $n$  [17]. This absorption was attributed to large polarons [6], and its softening was explained in terms of polaron-polaron interactions which increase with  $n$  [26,27]. At room temperature, where  $k_B T \approx \Delta$ , incoherent polaron hopping takes place: This may explain the flat background observed in Figs. 2(c) and 2(d) and the resulting, nonvanishing  $\sigma_{dc}$  at  $p < p_{MIT}$ . The above scenario is also consistent with recent calculations of the optical conductivity in hole-doped cuprates. They are based on a  $t$ - $J$  Holstein approach, where the FIR band has a dominant electron-phonon character, while the MIR band is attributed mainly to electron-spin interactions [28]. The observation of the MIR band at  $p > p_{MIT}$  therefore indicates that local antiferromagnetic fluctuations survive in the underdoped metallic state, as also reported previously for YBCO [29]. As  $p$  decreases, in Fig. 2,  $\omega_{MIR}$  shifts steadily to higher energies, to reach  $\sim 4500 \text{ cm}^{-1}$  at  $p \approx 0.015$ . This value is consistent with the determinations of the MIR peak in the other cuprates ( $\sim 0.5 \text{ eV}$ ) [30]. Despite that shift, in Fig. 2, the MIR absorption does not seem to play a major role in the MIT.

In conclusion, we have measured both the dc and infrared conductivity of BSLCO with different doping and of a lightly doped sample of YBCO. We have thus monitored the mechanism of the metal-to-insulator transition in the hole-doped Cu-O plane. For any  $p$  from 0.12 down to 0.015, we have detected a MIR band which hardens for decreasing  $p$  but is poorly sensitive to the MIT. In the far-infrared region, on the contrary, the Drude term of the metallic phase collapses at the MIT into a FIR band at finite frequency. As  $p$  is further decreased, this band shifts to higher energies, leaving behind a gap at low  $T$  and a flat absorption tail at high  $T$ . The FIR gap observed here is in quantitative agreement with that reported by ARPES in other cuprates with similar doping at low  $T$ , and the FIR peak frequency is correctly predicted by a simple Mott-transition model. Both bands identified here are consistent with a recent model, where the carrier localization is interpreted in terms of charge and spin polarons. According to this interpretation, the FIR band is mainly

due to electron-phonon interaction and the MIR band to electron-spin interaction.

We are gratefully indebted to Andreas Erb for providing the YBCO crystal. This work has been partially funded by PRIN 2005022492. S. O. was supported by KAKENHI No. 20740213.

- 
- [1] K. M. Shen *et al.*, Phys. Rev. B **69**, 054503 (2004).
  - [2] For a review, see T. Timusk and B. Statt, Rep. Prog. Phys. **62**, 61 (1999).
  - [3] Y. Iye, in *Properties of High Temperature Superconductors*, edited by D.M. Ginsberg (World Scientific, Singapore, 1992), Vol. 3, pp. 285–361.
  - [4] W. A. Atkinson and P.J. Hirschfeld, Phys. Rev. Lett. **88**, 187003 (2002).
  - [5] G. De Filippis, V. Cataudella, A. S. Mishchenko, and N. Nagaosa, Phys. Rev. Lett. **99**, 146405 (2007).
  - [6] For a review, see P. Calvani, Riv. Nuovo Cimento Soc. Ital. Fis. **24**, 1 (2001).
  - [7] S. Ono *et al.*, Phys. Rev. Lett. **85**, 638 (2000).
  - [8] Yoichi Ando *et al.*, Phys. Rev. B **61**, R14956 (2000); **63**, 069902(E) (2001).
  - [9] S. Ono and Yoichi Ando, Phys. Rev. B **67**, 104512 (2003).
  - [10] A. Jánossy, T. Fehér, and A. Erb, Phys. Rev. Lett. **91**, 177001 (2003).
  - [11] Yoichi Ando, J. Phys. Chem. Solids **69**, 3195 (2008).
  - [12] I. Terasaki *et al.*, Phys. Rev. B **41**, 865 (1990).
  - [13] A. Jánossy (private communication).
  - [14] S. Tajima *et al.*, Phys. Rev. B **43**, 10496 (1991).
  - [15] M. Hashimoto *et al.*, Phys. Rev. B **77**, 094516 (2008).
  - [16] A. Lucarelli *et al.*, Phys. Rev. Lett. **90**, 037002 (2003).
  - [17] S. Lupi *et al.*, Phys. Rev. Lett. **83**, 4852 (1999).
  - [18] T. Katsufuji *et al.*, Phys. Rev. Lett. **75**, 3497 (1995).
  - [19] W.J. Padilla *et al.*, Phys. Rev. B **72**, 060511(R) (2005).
  - [20] J. Meng *et al.*, Phys. Rev. B **79**, 024514 (2009).
  - [21] P. Calvani *et al.*, Solid State Commun. **91**, 113 (1994).
  - [22] N. Mott, in *Metal-Insulator Transitions* (Taylor & Francis, London, 1990).
  - [23] The three-dimensional Mott criterion can be extended to a charge moving in the Cu-O plane with small corrections, as shown by M. A. Kastner *et al.*, Rev. Mod. Phys. **70**, 897 (1998); in the present general approach, we adopted the simple geometrical factor  $1/\sqrt{\pi}$  instead of the usual, phenomenological value 0.25 which leads, for example, to a large mismatch with the  $p_{MIT}$  of Si:P [C. Kittel, *Introduction to Solid State Physics* (John Wiley and Sons, New York, 1996), 7th ed., p. 285].
  - [24] D.N. Basov, B. Dabrowski, and T. Timusk, Phys. Rev. Lett. **81**, 2132 (1998).
  - [25] D.N. Basov *et al.*, Phys. Rev. B **49**, 12165 (1994).
  - [26] J. Tempere and J.T. Devreese, Phys. Rev. B **64**, 104504 (2001); Eur. Phys. J. B **20**, 27 (2001).
  - [27] J. Lorenzana, Europhys. Lett. **53**, 532 (2001).
  - [28] A. S. Mishchenko *et al.*, Phys. Rev. Lett. **100**, 166401 (2008).
  - [29] Y. S. Lee *et al.*, Phys. Rev. B **72**, 054529 (2005).
  - [30] D.N. Basov and T. Timusk, Rev. Mod. Phys. **77**, 721 (2005).